

Quantum Information Scrambling Through a High-Complexity Operator Mapping

Xiaopeng Li,^{1,2} Guanyu Zhu,³ Muxin Han,⁴ and Xin Wang⁵

¹*State Key Laboratory of Surface Physics, Institute of Nanoelectronics and Quantum Computing, and Department of Physics, Fudan University, Shanghai 200433, China*

²*Collaborative Innovation Center of Advanced Microstructures, Nanjing 210093, China**

³*Joint Quantum Institute, NIST/University of Maryland, College Park, Maryland 20742, USA*

⁴*Department of Physics, Florida Atlantic University, 777 Glades Road, Boca Raton, FL 33431, USA*

⁵*Department of Physics, City University of Hong Kong,*

Tat Chee Avenue, Kowloon, Hong Kong SAR, China,

and City University of Hong Kong Shenzhen Research Institute, Shenzhen, Guangdong 518057, China

(Dated: December 14, 2022)

Recently, quantum information scrambling has attracted much attention amid the effort to reconcile the apparent conflict between quantum-mechanical unitarity and the irreversibility of thermalization in quantum many-body systems. Here we propose an unconventional mechanism to generate quantum information scrambling through a high-complexity mapping from logical to physical degrees of freedom that hides the logical information into non-separable many-body correlations. We develop an algorithm to compute all physical observables in dynamics with a polynomial-in-system-size cost. The system shows information scrambling in the quantum many-body Hilbert space characterized by the spreading of Hamming distance defined by a set of a natural orbital bases, which can also be calculated with a time polynomial in system size. Despite the polynomial complexity, the operator-mapping enabled growth in the out-of-time-order-correlator still exhibits quantum chaotic behavior. The information-hiding mapping approach opens up a novel venue to investigate fundamental connections among computational complexity, information scrambling and quantum thermalization.

Introduction

Recent developments in engineering synthetic quantum devices have achieved unprecedented controllability over a wide range of quantum degrees of freedom [1–7]. Theoretically, it has been realized that there is a fundamental difference between few- and many- qubit systems—a few-qubit system undergoing unitary evolution is easily reversible by a quantum circuit, whereas the reverse for many qubits is unarguably impossible due to quantum thermalization despite of unitarity [8–13]. This apparent conflict between unitarity and irreversibility with many qubits undermines our fundamental understanding of quantum thermalization in a closed quantum system. To reconcile the conflict, the eigenstate thermalization hypothesis has been formulated theoretically [8, 9] and confirmed numerically [14]. Nevertheless, the microscopic mechanism of the thermalization still remains mysterious. Amid the fast-growing research interests on synthetic quantum systems for the purposes of quantum information processing and beyond, a thorough understanding of this problem is key for the field of further progress [15, 16].

The problem of many-body unitarity also emerges in modeling the quantum effects of black holes [17]. The black hole information paradox and the recent firewall paradox have received enormous research interests in

the last few years [18–31]. Recent developments follow the idea of the holographic Anti-de Sitter/Conformal Field Theory (AdS/CFT) correspondence [32], employing boundary holographic models to describe the bulk quantum black hole. The holographic approach leads to an intriguing result: the black hole corresponds to quantum chaos and fast scrambling in the boundary holographic models [33]. The holographic chaos is mostly studied using the $0+1$ dimensional Sachdev-Ye-Kitaev (SYK) model [34, 35] and its variants owing to the exact-solvable nature in large- N limit [21, 26–29, 31] and the fast scrambling property. In addition, researchers are now approaching a consensus that the computational complexity underlying the quantum dynamical evolution of a many-body system plays a central role in understanding quantum chaos [36, 37], although a solid theoretical framework for that is still lacking.

Here we propose an alternative approach for quantum information scrambling by applying a high complexity mapping, which naturally goes beyond the $0+1$ dimension. In our proposed mechanism, despite that the quantum state follows integrable unitary evolution, quantum information is gradually lost in a physical setting, morphing into non-separable many-body correlations because of the high complexity of the mapping between integrals of motion and physical observables in the system. This mechanism is demonstrated by an exact solvable model of spinless hard core fermions [38]. We show that the system exhibits information scrambling in the exponentially-sized Hilbert space. This dynamical pro-

* xiaopeng_li@fudan.edu.cn

cess is quantified by a Hamming distance [39] defined by a set of natural orbital bases, which can be calculated with a polynomial time-cost for this model on a classical computer. Despite the relatively low computational time cost (polynomial) in calculating all equal-time observables, we still find that the physical system develops quantum chaotic growth in the out-of-time-order correlator (OTOC) [40]. The mapping-complexity in our proposed mechanism can be in principle generalized to more generic cases, which we expect to open up a wide window to investigate the fundamental interplay of computational complexity, thermalization and information scrambling.

Results

Quantum information scrambling through a high-complexity map. For a generic quantum system the time evolution of a physical observable \mathcal{O} is described by the expectation value of the Heisenberg operator $\mathcal{O}(t) = e^{iHt} \mathcal{O} e^{-iHt}$, with H the system Hamiltonian. Considering a quantum state $|\Psi\rangle$ with information encoded by a set of few-body observables as $\mathcal{O}_\alpha|\Psi\rangle = \lambda_\alpha|\Psi\rangle$ —for example these operators could be local pauli operators or stabilizers—its quantum evolution is deterministically given by $\mathcal{O}_\alpha(-t)|\Psi(t)\rangle = \lambda_\alpha|\Psi(t)\rangle$. Through this dynamical process the information becomes hidden into $\mathcal{O}_\alpha(-t)$, which are in general highly nonlocal many-body operators [31, 41–45]. Tracking the mapping $\{\mathcal{O}_\alpha\} \mapsto \{\mathcal{O}_\alpha(-t)\}$ for a generic Hamiltonian is exponentially complex, making the extraction of quantum information after long-time evolution practically impossible, i.e., quantum information scrambles with the time evolution. The scrambling process can thus be treated as quantum information initiated in few-body degrees of freedom hidden into non-separable many-body correlations through a high-complexity mapping.

It is evident that the $\mathcal{O}_\alpha(t)$ operators having a non-separable many-body nature is necessary for information scrambling, but it is unclear whether the mapping having an exponential complexity is also necessary or not. Finding a relatively lower-complexity mapping from few- to many-body operators that still causes information scrambling is not only of fundamental interest but would also assist in constructing exact models for nontrivial quantum many-body dynamics. In the following, we provide such a mapping based on spin-1/2 qubits.

Consider a one-dimensional spin chain, $\sigma_j^{x,y,z}$, with the site index $j \in [1, L]$. We assume that the total spin S_z component is conserved, and we shall work in the Hilbert space sector having $\sum_{j=1}^L \sigma_j^z/2 = S_z$. We introduce a highly nonlocal projective mapping as,

$$\begin{aligned} \tau_1^z &= \sigma_1^z P \\ \tau_{k \neq 1}^z &= \sum_{\vec{s}_k} \sigma_{k+\sum_{j=1}^{k-1} (s_j+1/2)}^z \mathcal{Q}_{\vec{s}}^k P \end{aligned} \quad (1)$$

where the two projectors are $P = \prod_{j=1}^{L-1} [4 - (\sigma_j^z + 1)(\sigma_{j+1}^z + 1)]$, $\mathcal{Q}_{\vec{s}}^k = \prod_{j=1}^{k-1} [s_j \tau_j^z + 1/2]$, with $\vec{s}_k = \{s_1, s_2, \dots, s_{k-1}\}$, $s_j = \pm 1/2$, $k \in [1, L_\tau]$, ($L_\tau \equiv L/2 + 1 - S_z$). Correspondingly, we have $\tau_k^+ \tau_{k'}^- = \sum_{\vec{s}_k} \sigma_{k+\sum_{j=1}^{k-1} (s_j+1/2)}^+ \mathcal{Q}_{\vec{s}}^k \sum_{\vec{s}_{k'}} \sigma_{k'+\sum_{j=1}^{k'-1} s'_j+1/2}^- \mathcal{Q}_{\vec{s}'}^{k'} P$, with $\sigma^\pm = (\sigma^x \pm i\sigma^y)/2$. These τ operators satisfy spin-1/2 algebra. We shall consider a quantum state with information encoded as $\tau_k^z|\Psi\rangle = (2m_k^0 - 1)|\Psi\rangle$, that undergoes dynamical evolution according to the Hamiltonian

$$H = \frac{1}{2} \sum_{k=1}^{L_\tau} [\tau_k^x \tau_{k+1}^x + \tau_k^y \tau_{k+1}^y]. \quad (2)$$

An open boundary condition is adopted in this work. In the σ basis, the system is still local, and we have $H = \frac{1}{2} \sum_{j=1}^L P [\sigma_j^x \sigma_{j+1}^x + \sigma_j^y \sigma_{j+1}^y] P$ and $\sigma_j^z|\Psi\rangle = (2n_j^0 - 1)|\Psi\rangle$.

The dynamics in this system is more transparent in the fermion picture through a Jordan-Wigner transformation, where we introduce f_k and c_j corresponding to τ and σ degrees of freedom, respectively. In the fermion picture, total S_z conservation implies that the total particle number $N (= S_z + L/2)$ is conserved. Corresponding to Eq. (2), f_k operators follow free fermion dynamics with a Hamiltonian $\sum_k (f_k^\dagger f_{k+1} + H.c.)$, and c_j follow dynamics of a spinless hard-core fermion model with infinite nearest neighbor interaction, whose ground state is shown to be an interacting Luttinger liquid [38]. To proceed, we introduce the natural orbital bases $C_j(t)$ associated with c operators by diagonalizing the time-dependent correlation function by

$$\langle \Psi(t) | c_j^\dagger c_{j'} | \Psi(t) \rangle = \sum_i \lambda_i(t) U_{j,i}^c(t) U_{j',i}^{c*}(t), \quad (3)$$

and $C_i = \sum_j U_{j,i}^c c_j$. The natural orbital bases associated with f operators are defined in the same way as F_k , which is given by $F_k(t) = e^{-iHt} f_k e^{iHt}$. During the dynamical evolution, the quantum information is thus stored as $F_k^\dagger F_k |\Psi(t)\rangle = m_k^0 |\Psi\rangle$, whereas in the σ bases (or equivalently the c bases) and the dynamical $\sigma_j^z(-t)$ operator holding the information has a non-separable many-body character. Mathematically, this dual feature allows us to track the quantum information with τ s, and at the same time study the interesting many-body quantum dynamics in the σ s. In the following, we assume physical access to the σ degrees of freedom, and will thus refer to τ and σ as logical and physical degrees of freedom, respectively. This dual feature is also expected to shed light on understanding operator growth in black hole scrambling physics [25, 31].

Computation complexity for the physical observables. Despite the many-body nature of the mapping

from the logical to physical qubits in Eq. (1), we find that the computational complexity to extract the physical observables is polynomial in the system size. For the dynamical quantum state, $|\Psi(t)\rangle = [F_k^\dagger(t)]^{m_k^0}|0\rangle$, the time-dependent wave function $\Psi_{\vec{m}}$ in the basis of $|\vec{m}\rangle = \prod_k [f_k^\dagger(0)]^{m_k}|0\rangle$ is a Slater-determinant. It is then straightforward to calculate the few-body observables in terms of the logical qubits via Wick theorem. However the Wick theorem does not carry over to observables composed of physical qubits. A direct calculation of the expectation value of such a physical observable \mathcal{O} , $\langle \mathcal{O} \rangle = \sum_{\vec{m}, \vec{m}'} \mathcal{O}_{\vec{m}\vec{m}'} \Psi_{\vec{m}}^*(t) \Psi_{\vec{m}'}(t)$, requires evaluating an exponentially large (in the system size) number of Slater-determinants, and is thus intractable for large systems. To overcome this difficulty, we develop an algorithm to explicitly sample the Slater determinants efficiently, through which the overall computation complexity to calculate one physical observable is reduced to $O(L\tau N^{3.373}/\delta^2)$, δ being the desired error threshold (see Methods). The dynamics for the interacting physical system defined by the mapping (Eq. (1)) is thus *almost* exactly solvable, in the sense that the computational complexity does not scale exponentially.

Likewise, the matrix elements of the dynamical many-body operator $\langle \vec{m} | e^{-iHt} c_j^\dagger c_j e^{iHt} | \vec{m}' \rangle$ holding the information in the physical basis, can be calculated at a time cost which scales polynomially, much more efficient than the exponential scaling in conventional settings.

Hamming distance as a measure for information scrambling. To quantify information scrambling from few- to many-body degrees of freedom, we generalize a previously introduced Hamming distance [39] to natural orbital occupation basis. In this basis, the Hilbert space is spanned by the time-dependent states $|\vec{n}; t\rangle = [C_1^\dagger]^{n_1} [C_2^\dagger]^{n_2} \dots |0\rangle$. The Hamming distance that characterizes the distance between the dynamical state and the initial state in the Hilbert space is

$$\mathcal{D}(t) = \sum_{\vec{n}} (\vec{n} - \vec{n}_0)^2 |\langle \vec{n}; t | \Psi(t) \rangle|^2, \quad (4)$$

where \vec{n}_0 represents the initial occupation of natural orbitals. This Hamming distance is also a measure of operator growth [31]. The natural orbital basis is defined by sorting the eigenvalues λ_j in descending order, so that $\lambda_{j \leq N} = 1$, and $\lambda_{j > N} = 0$ for the initial state, and $\lambda_j \geq \lambda_{j+1}$ in general. For systems that do not exhibit information scrambling such as free fermions or many-body localized systems, $\mathcal{D}(t)$ remains to be an intensive quantity in dynamics, i.e., $\mathcal{D}(t)/L \rightarrow 0$, whereas $\mathcal{D}(t)/L$ becomes finite at long-time when the information spreads over the Hilbert space.

A direct calculation of the Hamming distance is still exponentially difficult. We thus rewrite it in terms

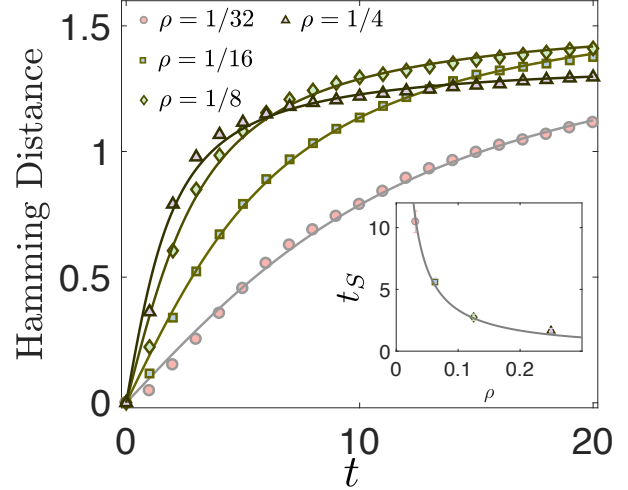


FIG. 1. Quantum information scrambling in Hilbert space measured by Hamming distance. In this figure, the shown Hamming distance is normalized by N . The system size is fixed to be 256 in this plot. We average over 10 random initial states and sampling 15000 states in Hilbert space to minimize the sampling error. The numerical results shown by symbol points fit to a function of $\arctan(t/t_S)$. The fitted form is shown by the lines in the plot. The characteristic time scale t_S exhibits a $1/\rho$ dependence as shown in the inset.

of observables as $\mathcal{D}(t) = 2N[1 - \chi(t)]$, with $\chi(t) = \frac{1}{N} \sum_l n_{0,l} \lambda_l$. Now the Hamming distance quantifying information spreading in the physical bases can be efficiently calculated at a polynomial time cost.

The results for Hamming distance are shown in Fig. 1. The information scrambling time t_S is determined by fitting the numerical results to $\mathcal{D}(t) = \mathcal{D}_\infty \arctan(t/t_S)$. We find that at long time limit \mathcal{D}_∞ is an extensive quantity, i.e., \mathcal{D}_∞/N is non-zero, and it approaches $2N(1 - \rho)$ as we increase total N , with the fermion density $\rho = N/L$. This means the quantum information encoded in the logical τ basis scrambles to the whole many-body Hilbert space in the σ basis. The scrambling time t_S , here referring to the time for the one-dimensional system to fully scramble, is found to have a $1/\rho$ dependence, which is qualitatively as expected because the effective interactions between physical fermions increase upon increasing the particle number density.

Correlation relaxation dynamics. Apart from Hamming distance, the quantum memory loss in the physical basis can also be seen in the relaxation dynamics of correlations. Fig. 2 shows the evolution of the natural orbital occupation numbers, which are obtained through the eigenvalues of the correlation matrix $\langle \Psi(t) | c_i^\dagger c_j | \Psi(t) \rangle$. In the dilute limit of $\rho \rightarrow 0$, the interaction effects are vanishing, and the system is essentially formed by non-

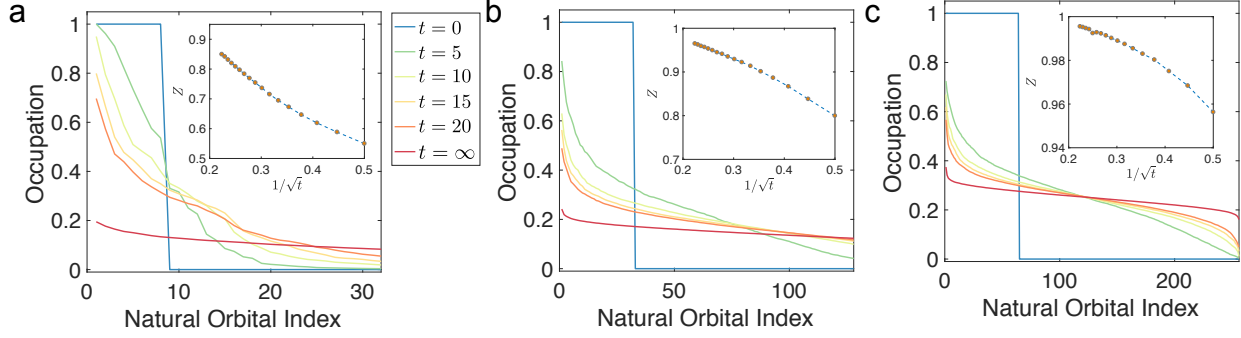


FIG. 2. Correlation relaxation dynamics of the physical degrees of freedom. (a, b, c) show the occupation numbers of natural orbital basis (see main text), with different $N = 8, 32, 64$, respectively. The total system size is fixed at $L = 256$. The $t = \infty$ results correspond to $t = 10^6$ in the calculation. Despite the logical degrees of freedom f_k are non-interacting, the physical ones show effective interaction effects in that natural orbital occupation exhibits relaxation behavior because otherwise they would not. The inset shows $Z(t)$ (see main text), which fits to a power law form of $1 - Z(t) = \sqrt{t_r/t} + O(1/L)$.

interacting fermions that do not relax. Away from that limit, we find efficient relaxation in the correlation, and the relaxation rate becomes stronger as we increase the particle number N . To quantify the relaxation dynamics, we introduce $Z(t) = \frac{1}{N} \sum_l \sqrt{\lambda_l(t) \lambda_l(t \rightarrow \infty)}$ that approaches 1 in the long-time limit.

We find that for large systems the long-time behavior in $Z(t)$ is captured by $1 - Z(t) = \sqrt{t_r/t} + O(1/L)$, which is attributed to diffusive dynamics. At a time t much longer than microscopic time scales, the system is formed by domains of fermions in a vacuum background. The typical domain size is expected to be \sqrt{Dt} , with D the diffusion constant. The late-time behavior determined by the domain-size growth would lead to the $1/\sqrt{t}$ relaxation (see Methods). This behavior also implies a fast scrambling of quantum information of the system, because otherwise the late-time dynamics would not be described by classical diffusion physics.

Operator-mapping enabled OTOC growth. Despite the polynomial time cost in calculating all equal-time observables, our physical system still exhibits quantum chaotic behavior in the OTOC [40] to be explained below. The correlator we use here takes a form of $G_{jj'}(t) = \langle \sigma_j^z(t) \sigma_{j'}^z(0) \sigma_j^z(t) \sigma_{j'}^z(0) \rangle_\beta$, with $\sigma_j(t)$ the Heisenberg operator, and $\langle \dots \rangle_\beta$ the thermal ensemble average. The sampling method we developed to calculate dynamics in few-body observables would breakdown in calculating OTOC at long time, because the sampling error would explode as $\sqrt{2^{3v_L t}/M_s}$, with M_s being the sampling number, and v_L the Lieb-Robinson bound velocity [41]. We thus evaluate OTOC with exact methods, and afford to simulate the dynamics up to a system size $L = 32$, with gpu techniques.

Figure 3 shows the results for OTOC where the scrambling of quantum information is confirmed. Effective

interaction effects among the physical fermions are revealed as the OTOC spreading behaves as “ball-like” instead of “shell-like”, which differentiates interacting and free fermions [18, 19]. This further confirms the information scrambling in this system. The early-time behavior of OTOC gives the Lyapunov exponent λ_L which exhibits a mild dependence of the temperature, similar to the situation in [46]. Besides, the butterfly velocity is found to be approximately equal to the sound velocity in the conformal field theory at low energy, and its implication to black hole physics is worth further investigation.

Given that the physical system exhibits quantum chaotic behavior and that the computational complexity for equal-time observables is polynomial in the system size, our quantum operator-mapping scheme is expected to motivate further researches on the minimal computational complexity for chaotic phenomena, which is of fundamental interest in understanding complex many-body systems.

Discussion

We have presented a novel mechanism for quantum information scrambling by hiding the information behind a highly nonlocal mapping, which relates the physical degrees of freedom to the logical ones holding the quantum information. A concrete operator mapping is provided to support this mechanism. We develop an algorithm to calculate physical observables, the complexity of which is polynomial in the system size. This allows us to simulate quantum dynamics of large systems. By calculating Hamming distance, correlation relaxation and out-of-time-order correlators in dynamics, we confirm the physical system exhibits quantum information scrambling despite the fact that the mapping enabling scrambling has much lower complexity than exponential. Our discovery offers a better understanding of computation complex-

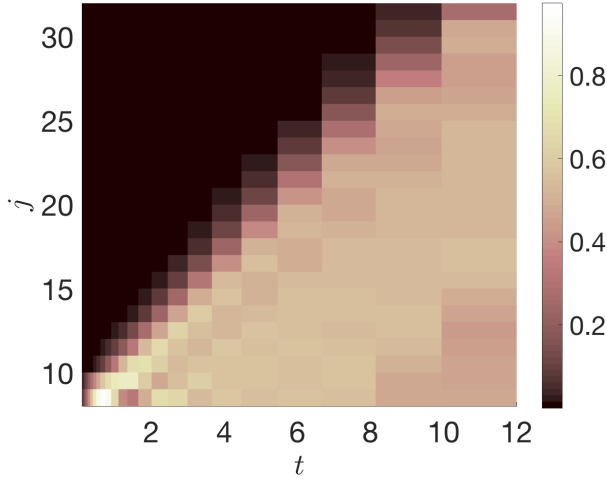


FIG. 3. Out-of-time-order correlator (OTOC) of the physical operators G_{ij} in dynamics. In dynamics, the correlator exhibits a light-cone behavior with a finite butterfly velocity. Once the operator separation range in OTOC is within the light-cone, they quickly scramble and locally equilibrate. In this figure, the temperature is fixed to be 1 here. In the calculation we choose system size $L = 32$ and $N = 8$. The color index the OTOC $G_{i=8,j}$ in this plot.

ity, quantum thermalization, and information scrambling, and the connections among them.

Practically, our approach gives novel ways to engineer models for quantum information steganography and quantum simulation benchmarking. For steganography, the unitary evolution $U(t)$ in our model resembles an encoding circuit in a quantum error correction code, which encodes logical information $\{\tau_j^z(t)\}$ non-locally in the physical basis starting from the information initialized locally in the physical basis $\{\sigma_j^z\}$. Therefore, there is no way to acquire information from local measurements, and the quantum information is hence hidden. Even other parties acquire the quantum memory, there is no way to easily read out the actual information without knowing the encoding scheme. The owner can vary the evolution time t in order to vary the encoding map. For the information owners, they will need a decoding circuit to recover the nonlocal quantum information into a local basis in order to use it or to read it out. The high-complexity mapping in Eq. (1) provides a better alternative for the decoding circuit than the straightforward approach of implementing a reverse circuit that has an exponential-decay-fidelity problem. For quantum simulation benchmarking, it is in general difficult to verify the quantum computer in simulating thermalization processes. Our proposing nonlocal mapping approach can be adapted to construct

models that exhibit nontrivial quantum dynamics and at the same time remains simulatable by a classical computer. Comparing results simulated by quantum and classical computers would help differentiate thermalization effects caused by equilibration of internal degrees of freedom from that by coupling to the external environment.

Furthermore our approach can be readily generalized to construct exact solutions for novel interacting quantum dynamics. Building nontrivial but tractable mappings from quantum integrable models may inspire ideas to formulate quantum Kolmogorov-Arnold-Moser theorem [47, 48], an important open question relevant to a broad range of physics spanning quantum chaos and quantum many-body localization.

Last but not least, we remark that the algorithm we developed to sample the Slater-determinant wave functions can also be used to improve efficiency in other contexts such as determinant quantum Monte Carlo, where the sampling is performed through a Markov chain approach. Our algorithm allows explicit and independent sampling without any autocorrelation.

Method

An efficient algorithm to sample Slater-determinant wave functions. A direct calculation of physical observables is exponentially difficult due to the highly nonlocal nature of mapping from the logical to the physical operators (Eq. (1)), despite the wave functions being simply Slater-determinant. We thus provide an explicit algorithm to sample the Slater determinants which do not require a calculation of exponentially large number of determinants. The algorithm is inspired by a recent work on boson sampling which proposes a sampling method for permanents [49]. Considering a Slater-determinant state represented by a matrix U where each column represents a single-particle wave function. The algorithm contains three steps. The first step is to generate a random permutation of the integer sequence $\vec{\eta} = [1, \dots, N]$, which has complexity $O(N)$. The generated sequence is denoted as a vector \vec{v} . The second step is to iteratively sample x_k (k is from 1 to N in the iteration) according to a conditional probability distribution $P(x_k | x_1, \dots, x_{k-1}; v_{k+1}, \dots, v_N) \propto \frac{1}{k!} |\text{Det} [U_{x_1 \dots x_k, \vec{\eta} \setminus v_{k+1}, \dots, v_N}]|^2$, with $\vec{\eta} \setminus v_{k+1}, \dots, v_N$ meaning to keep the elements in $\vec{\eta}$ after excluding $v_{k+1} \dots v_N$. Then choose an all zero vector \vec{m} and then set $m_{x_k} = 1$. The vector \vec{m} satisfies the required probability distribution $|\Psi_{\vec{m}}|^2$ because

$$\frac{1}{N!} \sum_{\vec{v}} \left[\prod_k P(x_k | x_1, \dots, x_{k-1}; v_{k+1}, \dots, v_N) \right] = |\Psi_{\vec{m}}|^2.$$

The sampling algorithm we developed substantially improves the calculation efficiency compared to the previ-

ously used approach in studying ground state Luttinger liquids [50], and allows to treat much larger system sizes.

Error and complexity analysis. The major cost to calculate the physical observables arises from sampling the determinants. In the algorithm provided above, the complexity for M_s samples scales as $O(M_s L \tau N^{z+1})$, with N^z the computational complexity to calculate the determinant of a $N \times N$ matrix ($z = 2.373$ with best known algorithm). Since the sampling error scales as $\varepsilon \sim 1/\sqrt{M_s}$, the computational complexity to calculate one physical observable is $O(\delta^{-2} L \tau N^{z+1})$, with δ the required error threshold.

Effective model for the $1/\sqrt{t}$ relaxation dynamics. In this section, we devise an effective model for the observed $1/\sqrt{t}$ relaxation of natural orbital occupation. Starting from random product states, the system is formed of fermion domains on top of a vacuum background, after certain microscopic time scales. Assuming diffusive dynamics, at time t the typical size of the domain goes is $l_d = \sqrt{Dt}$, with D the diffusion constant. With the randomly distributed domains, the central limit theorem implies that the fermion density $\langle c_j^\dagger c_j \rangle$ satisfies a normal distribution with a mean N/L and variance $\text{Var} = N/L(l_d^{-1} - L^{-1})$. The average of $\sqrt{\langle c_j^\dagger c_j \rangle}$ is then given as $\sqrt{N/L} \left[1 - \frac{1}{16} \frac{\text{Var}}{(N/L)^2} \right]$, from which we get $1 - Z(t) \sim \sqrt{t}$, after substitution of l_d by \sqrt{Dt} .

Acknowledgement

We acknowledge helpful discussion with Zhexuan Gong, Yuan-Ming Lu, Meng Cheng, and Sriram Ganeshan. This work is supported by National Program on Key Basic Research Project of China under Grant No. 2017YFA0304204 (XL), National Natural Science Foundation of China under Grants No. 117740067(XL), and the Thousand-Youth-Talent Program of China (XL). G.Z. is supported by US ARO-MURI and US YIP-ONR. M.H. acknowledges support from the US National Science Foundation through grant PHY-1602867, and the Start-up Grant at Florida Atlantic University, USA. X.W. acknowledges support from the Research Grants Council of the Hong Kong Special Administrative Region, China (No. CityU 11303617), the National Natural Science Foundation of China (No. 11604277), and the Guangdong Innovative and Entrepreneurial Research Team Program (No. 2016ZT06D348). This work was completed at the Aspen Center for Physics, which is supported by US National Science Foundation Grant PHY-1607611.

Author contributions

All authors worked on theoretical analysis and contributed in completing the paper.

Author information

The authors declare no competing financial interests. Correspondence and requests for material should be sent to xiaopeng.li@fudan.edu.cn. Supplementary information accompanies this paper.

-
- [1] Hammerer, K., Sørensen, A. S. & Polzik, E. S. Quantum interface between light and atomic ensembles. *Rev. Mod. Phys.* **82**, 1041–1093 (2010).
 - [2] Duan, L.-M. & Monroe, C. Colloquium: Quantum networks with trapped ions. *Rev. Mod. Phys.* **82**, 1209–1224 (2010).
 - [3] Xiang, Z.-L., Ashhab, S., You, J. Q. & Nori, F. Hybrid quantum circuits: Superconducting circuits interacting with other quantum systems. *Rev. Mod. Phys.* **85**, 623–653 (2013).
 - [4] Georgescu, I. M., Ashhab, S. & Nori, F. Quantum simulation. *Rev. Mod. Phys.* **86**, 153–185 (2014).
 - [5] Dutta, O. *et al.* Non-standard hubbard models in optical lattices: a review. *Reports on Progress in Physics* **78**, 066001 (2015).
 - [6] Li, X. & Liu, W. V. Physics of higher orbital bands in optical lattices: a review. *Reports on Progress in Physics* **79**, 116401 (2016).
 - [7] Wendin, G. Quantum information processing with superconducting circuits: a review. *Reports on Progress in Physics* **80**, 106001 (2017).
 - [8] Deutsch, J. M. Quantum statistical mechanics in a closed system. *Phys. Rev. A* **43**, 2046–2049 (1991).
 - [9] Srednicki, M. Chaos and quantum thermalization. *Phys. Rev. E* **50**, 888–901 (1994).
 - [10] Shaffer, D., Chamon, C., Hama, A. & Mucciolo, E. R. Irreversibility and entanglement spectrum statistics in quantum circuits. *Journal of Statistical Mechanics: Theory and Experiment* **2014**, P12007 (2014).
 - [11] Kaufman, A. M. *et al.* Quantum thermalization through entanglement in an isolated many-body system. *Science* **353**, 794–800 (2016). <http://science.sciencemag.org/content/353/6301/794.full.pdf>.
 - [12] Gärttner, M. *et al.* Measuring out-of-time-order correlations and multiple quantum spectra in a trapped-ion quantum magnet. *Nature Physics* **13**, 781 EP – (2017).
 - [13] Li, J. *et al.* Measuring out-of-time-order correlators on a nuclear magnetic resonance quantum simulator. *Phys. Rev. X* **7**, 031011 (2017).
 - [14] Rigol, M., Dunjko, V. & Olshanii, M. Thermalization and its mechanism for generic isolated quantum systems. *Nature* **452**, 854 EP – (2008).

- [15] Zhu, W., Botina, J. & Rabitz, H. Rapidly convergent iteration methods for quantum optimal control of population. *The Journal of Chemical Physics* **108**, 1953–1963 (1998).
- [16] Poggi, P. M. & Wisniacki, D. A. Optimal control of many-body quantum dynamics: Chaos and complexity. *Phys. Rev. A* **94**, 033406 (2016).
- [17] Almheiri, A., Marolf, D., Polchinski, J. & Sully, J. Black holes: complementarity or firewalls? *Journal of High Energy Physics* **2013**, 62 (2013).
- [18] Roberts, D. A. & Swingle, B. Lieb-robinson bound and the butterfly effect in quantum field theories. *Physical review letters* **117**, 091602 (2016).
- [19] Roberts, D. A., Stanford, D. & Susskind, L. Localized shocks. *Journal of High Energy Physics* **2015**, 51 (2015).
- [20] Aleiner, I. L., Faoro, L. & Ioffe, L. B. Microscopic model of quantum butterfly effect: out-of-time-order correlators and traveling combustion waves. *Annals of Physics* **375**, 378–406 (2016).
- [21] Gu, Y., Qi, X.-L. & Stanford, D. Local criticality, diffusion and chaos in generalized sachdev-ye-kitaev models. *Journal of High Energy Physics* **2017**, 125 (2017).
- [22] Chowdhury, D. & Swingle, B. Onset of many-body chaos in the $o(n)$ model. *Physical Review D* **96**, 065005 (2017).
- [23] Patel, A. A., Chowdhury, D., Sachdev, S. & Swingle, B. Quantum butterfly effect in weakly interacting diffusive metals. *Physical Review X* **7**, 031047 (2017).
- [24] von Keyserlingk, C., Rakovszky, T., Pollmann, F. & Sondhi, S. Operator hydrodynamics, otocs, and entanglement growth in systems without conservation laws. *arXiv preprint arXiv:1705.08910* (2017).
- [25] Nahum, A., Vijay, S. & Haah, J. Operator spreading in random unitary circuits. *arXiv preprint arXiv:1705.08975* (2017).
- [26] Gu, Y., Lucas, A. & Qi, X.-L. Spread of entanglement in a sachdev-ye-kitaev chain. *Journal of High Energy Physics* **2017**, 120 (2017).
- [27] Chen, Y., Zhai, H. & Zhang, P. Tunable quantum chaos in the sachdev-ye-kitaev model coupled to a thermal bath. *Journal of High Energy Physics* **2017**, 150 (2017).
- [28] Chen, X., Fan, R., Chen, Y., Zhai, H. & Zhang, P. Competition between chaotic and nonchaotic phases in a quadratically coupled sachdev-ye-kitaev model. *Phys. Rev. Lett.* **119**, 207603 (2017).
- [29] Jian, S.-K. & Yao, H. Solvable sachdev-ye-kitaev models in higher dimensions: From diffusion to many-body localization. *Phys. Rev. Lett.* **119**, 206602 (2017).
- [30] Xu, S. & Swingle, B. Accessing scrambling using matrix product operators. *arXiv preprint arXiv:1802.00801* (2018).
- [31] Roberts, D. A., Stanford, D. & Streicher, A. Operator growth in the SYK model. *ArXiv e-prints* (2018). 1802.02633.
- [32] Maldacena, J. M. The Large N limit of superconformal field theories and supergravity. *Int. J. Theor. Phys.* **38**, 1113–1133 (1999). [Adv. Theor. Math. Phys.2,231(1998)], hep-th/9711200.
- [33] Shenker, S. H. & Stanford, D. Black holes and the butterfly effect. *JHEP* **03**, 067 (2014). 1306.0622.
- [34] Sachdev, S. & Ye, J. Gapless spin-fluid ground state in a random quantum heisenberg magnet. *Physical review letters* **70**, 3339 (1993).
- [35] Kitaev, A. A simple model of quantum holography (2015).
- [36] Susskind, L. Black Holes and Complexity Classes. *ArXiv e-prints* (2018). 1802.02175.
- [37] Agón, C. A., Headrick, M. & Swingle, B. Subsystem Complexity and Holography. *ArXiv e-prints* (2018). 1804.01561.
- [38] Gómez-Santos, G. Generalized hard-core fermions in one dimension: An exactly solvable luttinger liquid. *Physical review letters* **70**, 3780 (1993).
- [39] Hauke, P. & Heyl, M. Many-body localization and quantum ergodicity in disordered long-range ising models. *Physical Review B* **92**, 134204 (2015).
- [40] Larkin, A. & Ovchinnikov, Y. N. Quasiclassical method in the theory of superconductivity. *Sov Phys JETP* **28**, 1200–1205 (1969).
- [41] Lieb, E. H. & Robinson, D. W. The finite group velocity of quantum spin systems. In *Statistical Mechanics*, 425–431 (Springer, 1972).
- [42] Hayden, P. & Preskill, J. Black holes as mirrors: quantum information in random subsystems. *Journal of High Energy Physics* **2007**, 120 (2007).
- [43] Sekino, Y. & Susskind, L. Fast scramblers. *Journal of High Energy Physics* **2008**, 065 (2008).
- [44] Hastings, M. B. Locality in quantum systems. *Quantum Theory from Small to Large Scales* **95**, 171–212 (2010).
- [45] Brown, W. G. & Viola, L. Convergence rates for arbitrary statistical moments of random quantum circuits. *Physical review letters* **104**, 250501 (2010).
- [46] Yao, N. Y. *et al.* Interferometric Approach to Probing Fast Scrambling (2016). arXiv: 1607.01801.
- [47] Kolmogorov, A. Preservation of conditionally periodic movements with small change in the hamilton function. In *Stochastic Behavior in Classical and Quantum Hamiltonian Systems*, 51–56 (Springer, 1979).
- [48] Fioretto, D. & Mussardo, G. Quantum quenches in integrable field theories. *New Journal of Physics* **12**, 055015 (2010).
- [49] Clifford, P. & Clifford, R. The classical complexity of boson sampling. In *Proceedings of the Twenty-Ninth Annual ACM-SIAM Symposium on Discrete Algorithms*, 146–155 (SIAM, 2018).
- [50] Cheong, S.-A. & Henley, C. L. Exact ground states and correlation functions of chain and ladder models of interacting hardcore bosons or spinless fermions. *Physical Review B* **80**, 165124 (2009).

Supplementary Information

S-1. NUMERICAL VERIFICATION FOR THE SAMPLING METHOD

To show the convergence in the sampling of the natural orbital occupation, we provide the results with different total number of samplings M_s in Fig. S1. It is found that the results already converge with $M_s = 14000$, and that increasing to $M_s = 28000$ does not make noticeable difference. In the main text, we use $M_s = 15000$.

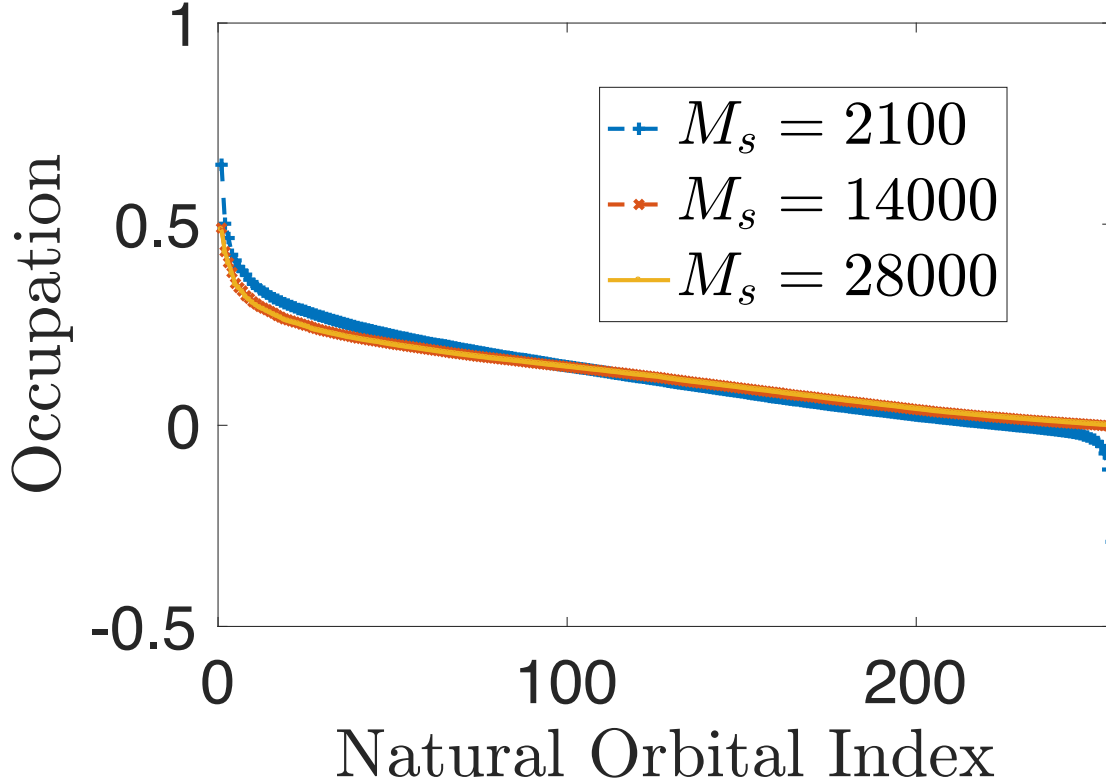


FIG. S1. Sampling convergence for the natural orbital occupation. This figure shows the natural orbital occupation at time $t = 20$ following the dynamics determined by the Hamiltonian in Eq. (2) starting from random initial states. From the results corresponding to different sampling number $M_s = 2100, 14000, 28000$, the results converge at the order of 10^4 .

S-2. INTERACTION EFFECTS IN THE GROUND STATE

To show the interaction effects in the hard core fermion model, we provide the momentum distribution of the ground state in Fig. S2, which matches the interacting Luttinger liquid theory with Luttinger parameter $K < 1$. In the dilute limit, the momentum distribution approaches to the free fermion case. Increasing the density, the decrease of the Luttinger parameter implies the increase of effective interactions.

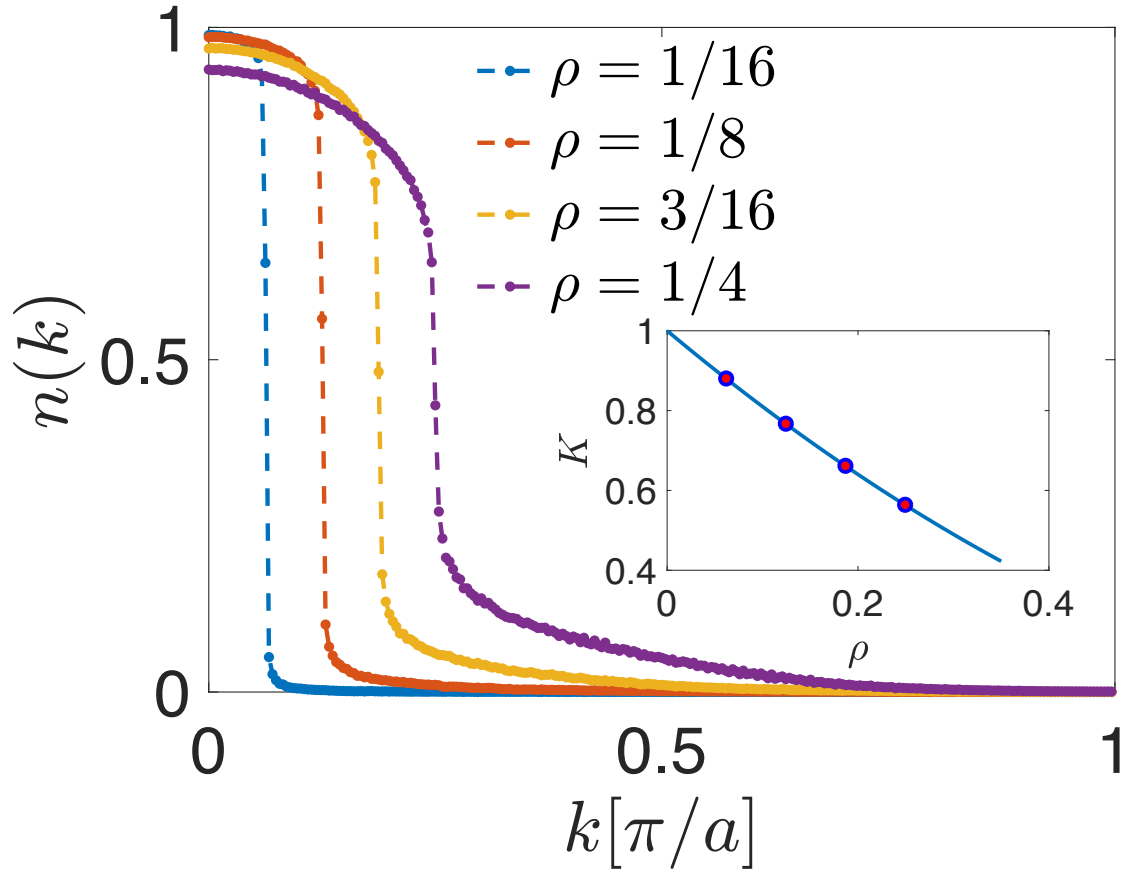


FIG. S2. Interaction effects in the model of hard-core spinless fermions. The momentum distribution $n(\mathbf{k})$ of the ground state is shown here, and it exhibits Luttinger liquid behavior. As we decrease the particle density, interaction effects become weaker, and the momentum distribution is approaching fermi-surface type. The interaction effects in this model can also be quantified by the deviation of the the ground state luttinger parameter K from the fermion case which has $K = 1$ (see the inset).